Nanocomposites Derived from a Low-Color Aromatic Polyimide (CP2) and Amine-Functionalized Vapor-Grown Carbon Nanofibers: In Situ Polymerization and Characterization

David H. Wang,[†] Michael J. Arlen,[‡] Jong-Beom Baek,[§] Richard A.Vaia,[||] and Loon-Seng Tan*,[||]

University of Dayton Research Institute, Dayton, Ohio 45469-0168, Department of Polymer Science, University of Akron, Akron, Ohio 44325, Department of Industrial Chemistry, Chungbuk National University, Chungbuk, 361-763, South Korea, and Polymer Branch, AFRL/MLBP, Materials & Manufacturing Directorate, Air Force Research Laboratory, Wright-Patterson AFB, Ohio 45433-7750

Received January 19, 2007; Revised Manuscript Received June 7, 2007

ABSTRACT: Vapor-grown carbon nanofibers (VGCNF) were functionalized with amine-containing pendants via a Friedel−Crafts acylation reaction with 4-(3-aminophenoxy)benzoic acid. The resulting H_2N−VGCNF with relatively high degree of functionalization was in attendance during the synthesis of a polyimide (previously designated as CP2) from 2,2-bis(phthalic anhydride)-1,1,1,3,3,3-hexafluoroisopropane (6FDA) and 1,3-bis(3-aminophenoxy)benzene (APB) in *N,N*-dimethylacetamide (DMAc). Thus, a series of CP2-based nanocomposite films, which contained 0.18−9.19 wt % of H_2N−VGCNF (corresponding to 0.10−5.0 wt % of basic VGCNF) were obtained using the conventional poly(amic acid) precursor method. For comparison purposes, the pristine VGCNF (0.10−5.0 wt %) was also used in the in situ polymerization of 6FDA and ABP. These two series of nanocomposite films were cast from the respective poly(amic acid)/VGCNF/DMAc solutions, followed by thermal imidization at curing temperatures up to 250 °C. The benefit and limitation of functionalized VGCNF on the length scale and the extent of CNF dispersion in a polyimide matrix were clear: (a) 0.18 wt % H_2N−VGCNF-*g*-CP2 film was visually transparent whereas a similarly prepared (0.10 wt %) VGCNF/CP2 film showed the presence of large CNF aggregates throughout; (b) at 0.55 wt % H_2N−VGCNF (equivalent to 0.30 wt % VGCNF) content, the nanocomposite film had become translucent, and at 9.19 wt % (equivalent to 5.0 wt % VGCNF), it was opaque. Since CP2 is very soluble in THF, the CP2-grafted VGCNF were simply separated from the free CP2 by solvent extraction. The molecular weights of the extracted CP2 were measured using gel-permeation chromatography (GPC). The effects of VGCNF on molecular weight (MW) and glass-transition (T_g) were discussed in terms of GPC and thermal analysis results, respectively. The dispersion of VGCNF in CP2 was evaluated using scanning electron microscopy (SEM). The tensile properties of these nanocomposite films were determined, showing up to 45% increase in modulus.

Introduction

One-dimensional, carbon-based nanomaterials can be broadly classified according to their diameter dimensions as follows: (i) single-wall carbon nanotube or SWNT (0.7−3 nm); (ii) multiwall carbon nanotube or MWNT (2−20 nm); (iii) carbon nanofiber or CNF (40−100 nm).[1] From the morphological standpoint, an important distinction among them is that while SWNT is a near-perfect graphene cylinder and MWNTs are made up by well-organized, cylindrical graphene layers, the turbostratic structure of CNFs lacks the perfection of graphene sheets. However, since the hollow structure of CNF is also made up of concentric graphene layers, it may be considered as MWNT when its average diameter is less than 100 nm.[2] In comparison to SWNT or MWNT, CNF is more attractive for its relatively low cost and availability in larger quantities as the result of their more advanced stage in commercial production. However, while there is a more widespread interest in the functionalization chemistry of SWNT and MWNT in the materials research community with the common objective of improving their dispersibility/solubility in organic solvents or aqueous media and optimizing the nanoscale dispersion and interfacial adhesion in solid matrices.[3−9] There are only relatively few reports on the chemical modification of CNF.[10,11]

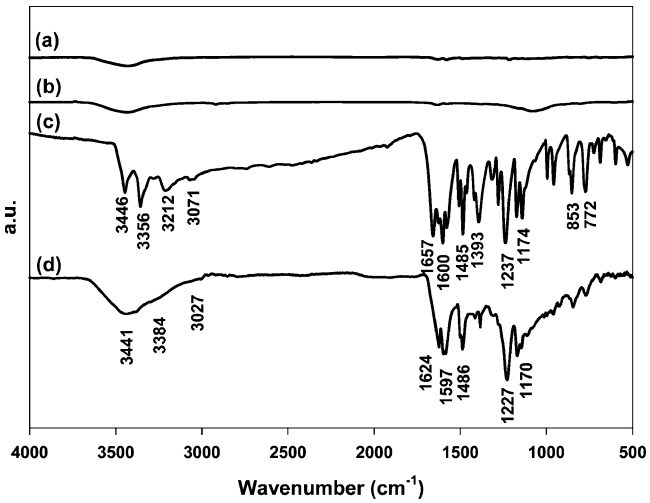

Figure 1. FT-IR spectra of (a) pristine VGCNF, (b) PT-VGCNF, (c) 3-aminophenoxy-4-benzoic acid (**4**) and (d) H_2N−VGCNF (**6**).

Recently, we have developed an effective method to directly arylcarbonylate vapor-grown carbon nanofibers (VGCNF) via

* Corresponding author. E-mail: loon-seng.tan@wpafb.af.mil. Voice mail: (937) 255-9141. Fax: (937) 255-9157.
[†] University of Dayton Research Institute.
[‡] Department of Polymer Science, University of Akron.
[§] Department of Industrial Chemistry, Chungbuk National University.
[||] Polymer Branch, AFRL/MLBP, Materials & Manufacturing Directorate, Air Force Research Laboratory.

10.1021/ma070157c CCC: $37.00
Published on Web 07/26/2007

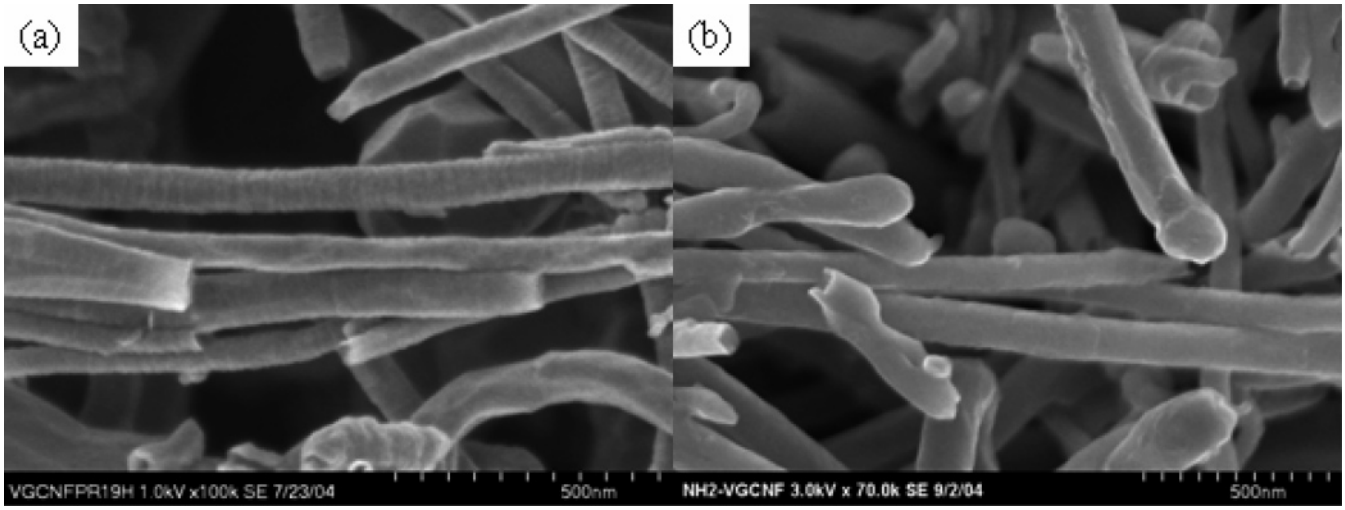

Figure 2. SEM images of (a) as-received VGCNF (×100K) and (b) H_2N-VGCNF (×70K).

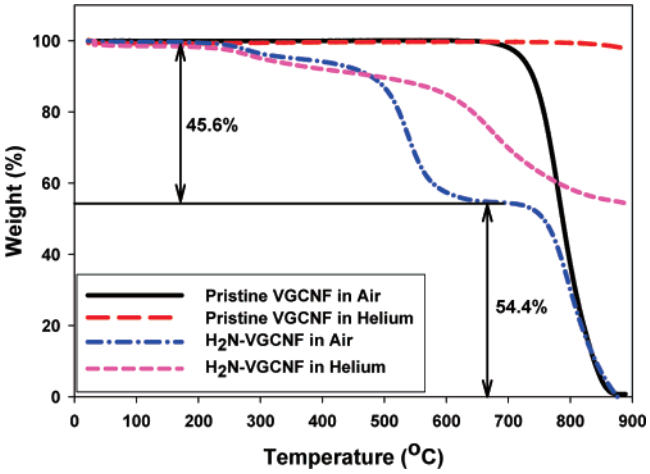

Figure 3. TGA thermograms with heating rate of 10 °C/min of pristine VGCNF and H_2N-VGCNF.

Friedel−Crafts (F−C) acylation reaction in poly(phosphoric acid) (PPA) with aromatic carboxylic acids, and also applied the technique to graft a linear poly(ether ketone) or a hyperbranched poly(ether ketone) onto pristine CNF/carbon nanotube (CNT) to generate the so-called in situ nanocomposites in a one-pot fashion.[10] Subsequently, in addition to extending the applicability of this functionalization method to MWNT, we have found useful functionalities such as OH and NH_2 to be chemically unaffected in the PPA-promoted F−C acylation. The VGCNF or MWNT prefunctionalized with these reactive groups would permit investigation into their effects on the in situ polymerization process and the resulting nanocomposites prepared in a two-stage fashion. Specifically, NH_2-functionalized CNF/CNT would be valuable in the preparation of polyimide-based nanocomposites. Polyimides display a unique combination of excellent mechanical, electrical and optical properties and outstanding thermal stability. Their monomers are readily available or relatively easy to prepare compared to those of other high performance polymers. Thus, polyimides have found many applications in high performance films and fibers, coatings, microelectronics, optoelectronics, adhesives, aerospace, nonlinear-optical devices, light-wave guide materials, and liquid crystal displays.[12] The polyimide, which is known as CP2[13] and derived from 2,2-bis(phthalic anhydride)-1,1,1,3,3,3-hexafluoroisopropane (6FDA) and 1,3-bis(3-aminophenoxy)benzene (APB) was selected for this work, primarily because of the extensive preparation and characterization studies that have been conducted on the nanocomposites of this polyimide and CNF/CNT. Thus, the pertinent synthesis, dispersion and property data are available for comparison.[14]

Experimental Section

Materials. Vapor grown carbon nanofiber (VGCNF, PR-19-HT) was obtained from Applied Science Inc., Cedarville, OH. VGCNFs are produced by a vapor-phase catalytic process in which a carbon-containing feedstock (e.g., CH_4, C_2H_4, etc.) is pyrolyzed in the presence of small metal catalyst (e.g., ferrocene, $Fe(CO)_5$, etc.). They have an outer diameter of 60−200 nm, a hollow core of 30−90 nm, and length on the order of 50−100 μm.[1,15,16] All other chemicals were reagent-grade and purchased from Aldrich Chemical Inc. and used as received, unless otherwise specified. *N*-Methyl-2-pyrrolidinone (NMP) was distilled under reduced pressure over phosphorus pentoxide. Anhydrous DMAc and other solvents were used as received. 2,2-bis(phthalic anhydride)-1,1,1,3,3,3-hexafluoroisopropane (6FDA; ≥99%) was purchased from Aldrich and used as received. 1,3-bis(3-aminophenoxy)benzene (ABP) was (99% min) was purchased from Chriskev Company, Inc.[17] and used as received.

Instrumentation. Proton and carbon nuclear magnetic resonance (^{1}H NMR and ^{13}C NMR) spectra for intermediates, monomer, and polymers were run at 270 and 50 MHz, respectively, on a Jeol-270 spectrometer. Infrared (IR) spectra were recorded on a Nicolet Nexus 470 Fourier transform spectrophotometer. Elemental analysis and mass spectral analysis were performed by System Support Branch, Materials Directorate, Air Force Research Lab, Dayton, Ohio. The melting points (mp) of all compounds were determined on a Mel-Temp melting point apparatus and are uncorrected. Intrinsic viscosities were determined with Cannon-Ubbelohde No. 75 viscometer. Flow times were recorded in NMP solution and polymer concentrations were approximately 0.5−0.10 g/dL at 30.0 ± 0.1 °C. Lithium bromide (1.0 wt %) was added to the solution to eliminate polyelectrolyte effect. Differential scanning calorimetry (DSC) analysis were performed in nitrogen with a heating rate of 10 °C/min using a Perkin-Elmer model 2000 thermal analyzer equipped with differential scanning calorimetry cell. Themogravimetric analysis (TGA) was conducted in nitrogen (N_2) and air atmospheres at a heating rate of 10 °C/min using a TA Hi-Res TGA 2950 themogravimetric analyzer. Gel permeation chromatography (GPC) was carried out on an Agilent 1100 Series equipped with refractive index and light scattering detectors. Tetrahydrofuran (THF) was used as the eluting solvent. The scanning electron microscope (SEM) used in this work was a Hitachi S-5200. Tensile strength and moduli of the polyimide films were tested using Tinius Olsen H10K-S Benchtop Testing Machine with a crosshead separation speed of 1 mm/min. Sonication was conducted at 20 kHz with a 600 W power using Ace Glass GEX 600−5 Ultrsonic Processor.

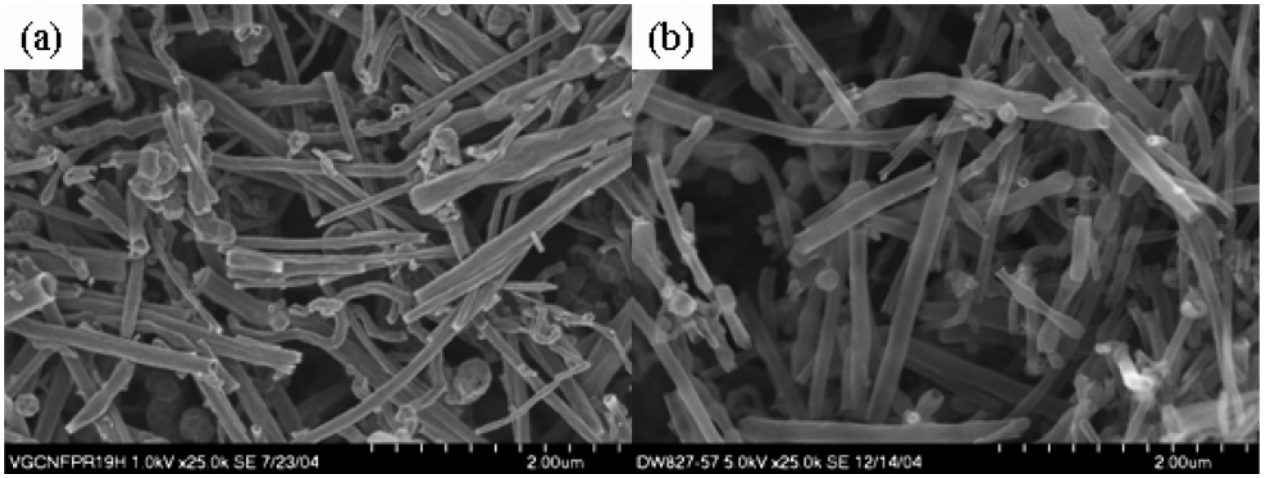

Figure 4. SEM images of (a) as-received VGCNF (×25K) and (b) PT-VGCNF (×25K).

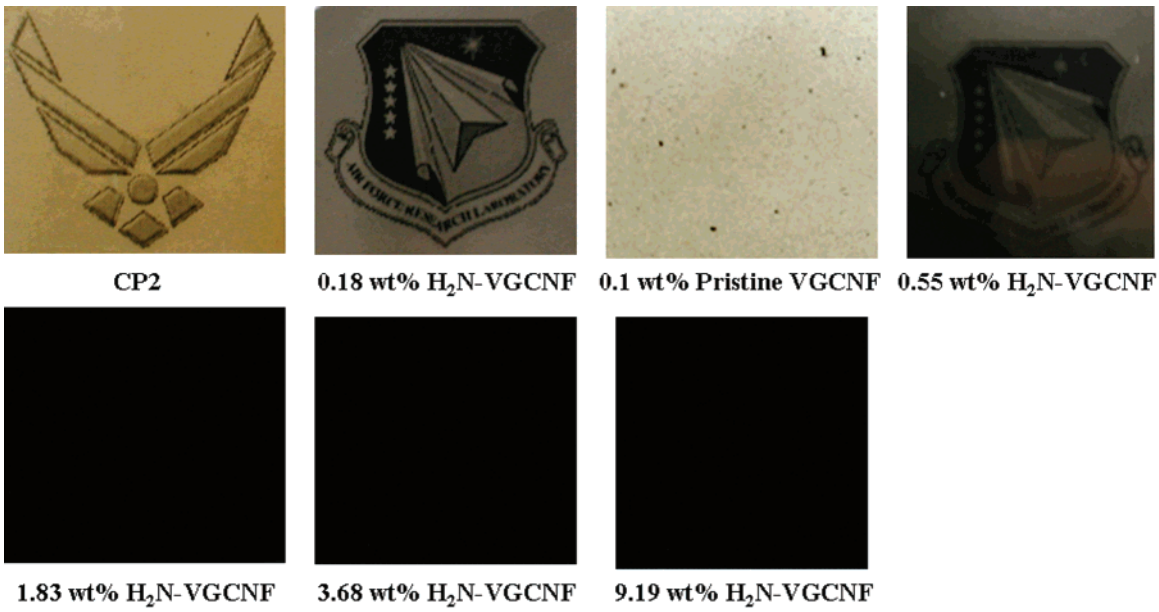

Figure 5. Visual comparison of film transparency in the unfilled CP2 film and films derived from the in situ nanocomposites with various amounts of amine-functionalized VGCNF (H_2N-VGCNF) and an in situ blend containing 1 wt % unfunctionalized VGCNF. Note that the amine functions on H_2N-VGCNF (used as labels for the photos above) should have been consumed during the in situ polymerization process.

4-(3-Aminophenoxy)benzonitrile (3).[18] Into a 250 mL three-necked flask equipped with a magnetic stirrer, a Dean−Stark trap, a nitrogen inlet and outlet, 4-nitrobenzonitrile (**1**; 7.41 g, 50.0 mmol), 3-aminophenol (**2**; 5.46 g, 50 mmol), potassium carbonate (8.28 g, 60.0 mmol), NMP (100 mL), and toluene (50 mL) were charged and stirred with dried nitrogen purging at 160 °C for 6 h. The mixture was allowed to cool to room temperature and filtered. The filtrate was poured into water. The white solid was collected by filtration and dried. It was dissolved in acetone and precipitated into water to afford 8.18 g (78% yield) of white solid, mp 88−90 °C (Lit.[18a] 84−88 °C). Anal. Calcd for $C_{13}H_{10}N_2O$: C, 74.27; H, 4.79; N, 13.32. Found: C, 74.09; H, 4.86; N, 13.35. FT-IR (KBr, cm^{-1}): 3486, 3392 (NH_2), 2218 (nitrile), 1629 (carbonyl). Mass spectrum (*m*/*e*): 210 (M^+). ^{1}H NMR (DMSO-d_6, δ in ppm): 5.38 (s, 2H, N***H***$_2$), 6.22−6.25 (dd, 1H, Ar−***H***), 6.30−6.32 (t, 1H, Ar−***H***), 6.46−6.50 (dd, 1H, Ar−***H***), 7.06−7.12 (m, 3H, Ar−***H***) and 7.80−7.83 (d, 2H, Ar−***H***). ^{13}C NMR (DMSO-d_6, δ in ppm): 104.59, 105.05, 106.90, 110.83, 117.91, 118.86, 130.48, 134.48, 150.89, 155.37, 161.44.

4-(3-Aminophenoxy)benzoic Acid (4).[19] Into a 100 mL three-necked flask, equipped with a magnetic stirrer, a nitrogen inlet and outlet, were charged 4-(3-aminophenoxy)benzonitrile (5.00 g, 24.0 mmol), polyphosphoric acid (83% P_2O_5 assay, 30.0 g) and water (5.30 g, 60.0 mmol), and the mixture was stirred with dried nitrogen purging at 120 °C for 8 h. The mixture was poured into water and the yellow solid was collected by filtration. It was recrystallized in water/ethanol (50:50) mixture to afford 4.50 g (83% yield) of yellow crystals, mp 145−147 °C (lit.[19] 145−147 °C). Anal. Calcd for $C_{13}H_{10}N_2O$: C, 68.11; H, 4.84; N, 6.11. Found: C, 68.36; H, 4.90; N, 6.23. FT-IR (KBr, cm^{-1}): 3446, 3356 (NH_2), 2500−3500 (broad, OH stretch in COOH), 3212, 3071, 1657 (carbonyl), 1600, 1485, 1393, 1237, 1174, 853, 772. Mass spectrum (*m*/*e*): 229 (M^+). ^{1}H NMR (DMSO-d_6, δ in ppm): 6.21−6.24 (dd, 1H, Ar−***H***), 6.27−6.28 (t, 1H, Ar−***H***), 6.41−6.45 (dd, 1H, Ar−***H***), 6.99−7.09 (m, 3H, Ar−***H***) and 7.92−7.95 (d, 2H, Ar−***H***). ^{13}C NMR (DMSO-d_6, δ in ppm): 104.81, 106.74, 110.32, 117.14, 124.68, 130.23, 131.44, 150.47, 155.74, 161.18, 166.71.

Functionalization of VGCNF with 3-aminophenoxy-4-benzoic acid (6, H_2N-VGCNF): Into a 250 mL resin flask equipped with a high torque mechanical stirrer, and nitrogen inlet and outlet, 3-aminophenoxy-4-benzoic acid (0.50 g, 2.18 mmol) and VGCNF (0.50 g), PPA (83% P_2O_5 assay, 20 g) and phosphorus pentoxide (P_2O_5, 5.0 g) were charged and stirred with dried nitrogen purging at 130 °C for 72 h. After cooling down to room-temperature water was added. The resulting precipitate was collected, washed with diluted ammonium hydroxide and Soxhlet extracted with water for 3 days and methanol for 3 days. It was then dried over P_2O_5 under reduced pressure at 100 °C for 72 h to afford 0.80 g (83% yield)

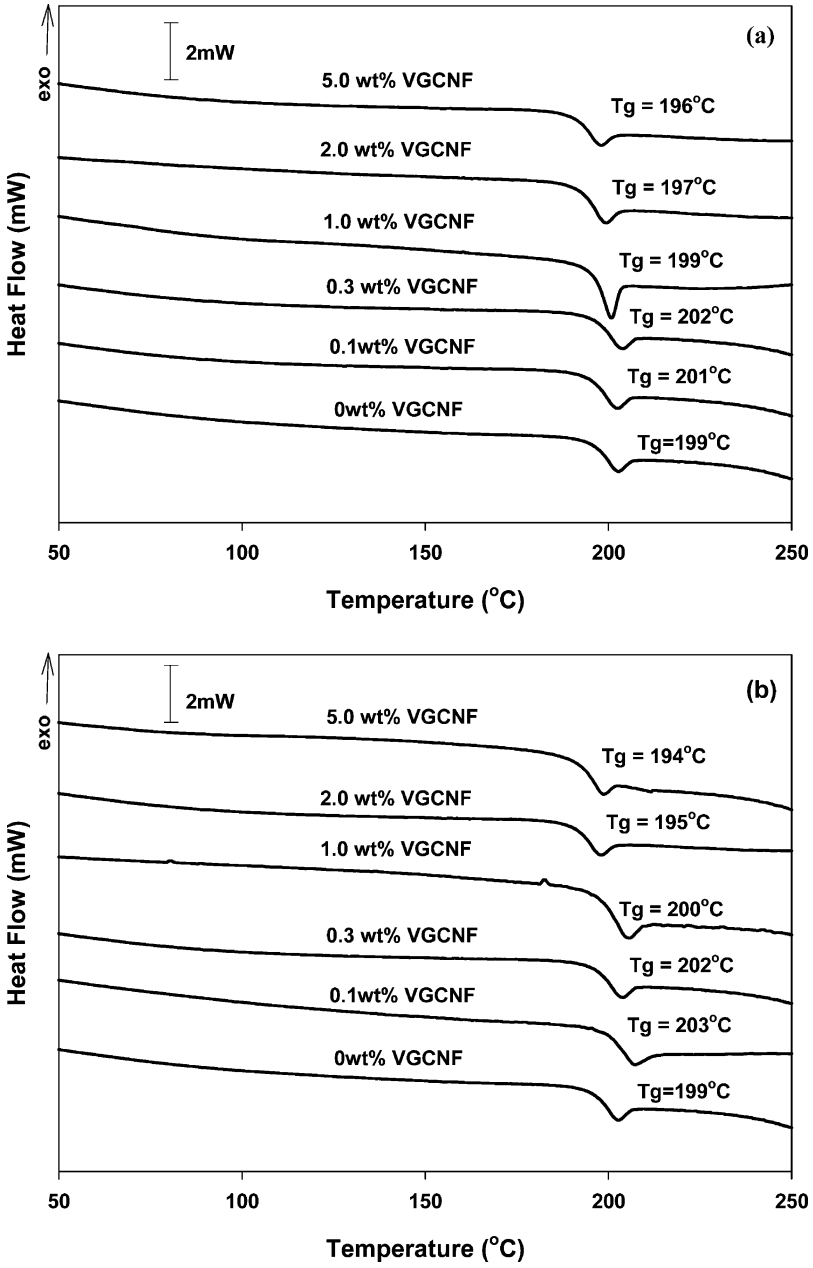

Figure 6. DSC thermograms of (a) CP2-*g*-VGCNF nanocomposites, and (b) CP2/VGCNF blends with heating rate of 10 °C/min.

of dark brown solid. Anal. Calcd For $C_{165}H_{50}N_5O_{10}$ (based on the assumption that for every 100 carbon, there are 5 3-aminophenoxy-4-benzoyl groups attached): C, 87.60; H, 2.11; N, 3.10; O, 7.07. Found: C, 87.11; H, 2.33; N, 3.43; O, 6.40. FT-IR (KBr, cm^{-1}): 3441, 3008, 1624 (carbonyl), 1597, 1486, 1227, 1170.

PPA-Treated VGCNF (7, PT-VGCNF): As a control experiment, the as-received VGCNF (0.50 g) together with poly(phosphoric acid) (PPA; 83% P_2O_5 assay; 20 g) and phosphorus pentoxide (P_2O_5, 5.0 g) were subjected to the same functionalization conditions and workup procedure that were used for H_2N-VGCNF to afford 0.47 (94% yield) of a black solid, designated as PT-VGCNF. Anal. Found: C, 98.66; H, 0.93; N, <0.20; O, <0.10.

Representative Preparation of CP2-*g*-VGCNF in Situ Nanocomposites (CP2 with 1.0 wt % H_2N-VGCNF Load). Into a 50 mL three necked flask equipped with a magnetic stirrer, nitrogen inlet and outlet, H_2N-VGCNF [**3**, 45.0 mg, which is equivalent to 28.3 mg (1 wt %) of unfunctionalized VGCNF] and anhydrous DMAc (20 mL) were placed and sonicated for 30 min until the H_2N-VGCNF was dispersed in NMP homogenously. 6FDA (1.777 g, 4.0 mmol) was added and stirred under dry nitrogen at room temperature for 30 min. Then APB (1.158 g, 3.96 mmol) was charged. The dark mixture was agitated at room temperature for 24 h to afford a viscous poly(amic acid) (PAA). The resulting mixture was diluted with DMAc (20 mL), poured into a glass dish, followed by vacuum evaporation of DMAc and heat-treatment at 100 °C/24 h; 150 °C/4h; 200 °C/2 h and 250 °C/1 h. The film thickness is about 0.1 mm. FT-IR (KBr, cm^{-1}): 3442, 3087, 1785, 1718 (imide), 1587, 1477, 1365, 1429, 1187, 1096, 962, 855.

Representative Preparation of CP2/VGCNF Blends via in Situ Polymerization of 6FDA and APB. (CP2 with 1.0 wt % As-Received VGCNF Load). The film of 1 wt % CP2/VGCNF blend (13) was prepared from 6FDA (1.777 g, 4.0 mmol), APB (1.158 g, 3.96 mmol), and as-received VGCNF (28.3 mg) using the same procedure used for CP2-*g*-VGCNF (**11**). The film thickness is about 0.1 mm. FT-IR (KBr, cm^{-1}): 3443, 3088, 1786, 1717 (imide), 1587, 1477, 1365, 1429, 1186, 1095, 855.

The Extraction of CP2 from the Cast Films 11 and 13. The weighed films were submerged in THF in closed sample vials at room temperature for over a 2-day period. During this period, the top part of the clear solution in each vial was taken out by a pipet, and the vials were then replenished with fresh THF. The above extraction routine was repeated more than 5 times until TLC showed

Table 1. Elemental Analysis Data for Pristine and Functionalized VGCNF

sample	anal.	C (%)	H (%)	N (%)	O (%)
pristine VGCNF	calcd	100	0	0	0
	found	99.02	1.01	<0.20[a]	<0.10[a]
H_2N-VGCNF	calcd[b]	87.60	2.23	3.10	7.07
	found	87.11	2.33	3.43	6.40
PT-VGCNF	calcd	100	0	0	0
	found	98.66	0.93	<0.20[a]	<0.10[a]

[a] Less than detection limit. [b] The empirical formula for H_2N-VGCNF, $C_{165}H_{50}N_5O_{10}$, is based on the assumption that for every 100 carbons there are five 4-(3-aminophenoxy)benzoyl groups attached, according to an estimate based on the TGA (air) result. The empirical formula of 4-(3-aminophenoxy)benzoyl group is $C_{13}H_{10}NO_2$. The calculation is based on the following equation: "theoretical weight loss at 700 °C" = $(n \times MW_{amine})/(100 \times AW_c + n \times MW_{amine}) \times 100$ where n is the number of 4-(3-aminophenoxy)benzoyl groups attached to VGCNF per 100 carbons. MW_{amine} is the molecular weight of 4-(3-aminophenoxy)benzoyl group, which is 212.22. AW_c is the atomic weight of carbon, which is 12.01. When n is equal to 5, the "theoretical weight loss at 700 °C" is 46.9% based on the above equation. This value is in good agreement with the weight loss at 700 °C (45.6%).

no sign of extracted free CP2 in THF. The residual powder or film (see Figure 6 and Figure SS-2, Supporting Information) was recovered and dried under vacuum overnight before weighing.

Results and Discussion

Synthesis and Characterization of H_2N-VGCNF. The diameter and length of the VGCNF (Pyrograf III-19-HT) used in this work were in the ranges of 60−200 nm and 5−30 μm, respectively. It follows that having aspect ratios (length/diameter) in the range of 100−600 should make them useful as nanolevel reinforcement for polymeric matrices. Furthermore, since their inherent electrical and thermal transport properties are also excellent, there are many application possibilities for tailoring their polymer−matrix composites into affordable, lightweight, multifunctional materials.

These VGCNF were heat-treated up to 3000 °C to graphitize the surface carbon, remove residual iron catalyst, and improve the associated conducting properties. The as-received (pristine) VGCNF contains 1.01 wt % of hydrogen as determined by elemental analysis (Table 1), presumably attributable to the sp^3 C−H and sp^2 C−H defects as methane is used as the major component in the feedstock for its production. On the basis of hydrogen content, there is approximately 11.5 atom % of C−H defects in VGCNF. These defects would provide sites susceptible to the electrophilic substitution (Friedel−Crafts acylation) reaction.[6]

The amine-containing acylating agent, namely, 3-aminophenoxy-4-benzoic acid (**4**) was prepared using a two-step synthetic route (Scheme 1). The nucleophilic nitro-displacement of 4-nitrobenzonitrile (**2**) with 3-aminophenol (**1**) in the presence of potassium carbonate yielded 3-aminophenoxy-4-benzonitrile (**3**), which was subsequently hydrolyzed in 100% of phosphoric acid to afford 3-aminophenoxy-4-benzoic acid (**4**).

On the basis of the results of our previous work on the model-compound and related in situ polymerization studies, we have reported that Friedel−Crafts (F−C) acylation in poly(phosphoric acid) (PPA) is a viable, alternative route to effecting a controlled functionalization of VGCNF and MWNT.[6] Thus, VGCNF and MWNT were not only functionalized with the aid of 2,4,6-trimethylphenoxybenzoic acid (TMPBA) as a model compound to probe, validate and quantify the extent of surface modification, but also were grafted with *m*-poly(ether ketone) (*m*PEK) and hyperbranched PEK via in situ polymerization with appropriate AB and AB_2 monomers using optimized PPA conditions that we previously described.[20] On account of the significant hydrogen content analyzed in the starting VGCNF and MWNT, it was concluded that the covalent attachment of the arylcarbonyl groups most probably occurred at the sp^2 C−H sites.

Amine functionality is one of the most versatile groups in polymer chemistry and various efforts have been reported to modify carbon nanosurfaces with amino groups.[21] In order to functionalize VGCNF with an amine group, we rationalized that amine group should be deactivated upon protonation in PPA and would not interfere with the intended F−C acylation reaction. Thus, we selected compound **4**, (3-aminophenoxy-4-benzoic acid),[19] a simple acylating agent containing both carboxylic acid and amine groups. Subsequently, VGCNF was treated with **4** at 130 °C in PPA/P_2O_5 via F−C acylation to afford an amine-functionalized VGCNF (H_2N-VGCNF, **6**) as shown in Scheme 1. Compound **4** exhibits carboxylic carbonyl stretches at 1657 cm^{-1} and a broad band at 2500−3500 cm^{-1}. The vibration bands of primary amine appear at 3446 (asym) and 3356 (sym) cm^{-1}. After F−C reaction, the carbonyl absorption of **6** is shifted to 1624 cm^{-1} as expected. The broad band at 2500−3500 cm^{-1}, which is associated with the hydroxyl stretch of carboxylic acid, has disappeared. The amine absorption becomes weak "spikes" at 3441 and 3384 cm^{-1}, sitting on top of the broad band attributable to the absorbed water in the KBr (Figure 1). These observed changes in the IR spectra indicate a successful grafting reaction. Furthermore, the scanning electron microscopy (SEM) revealed that the pristine VGCNF exhibits smooth textures on the surface whereas the rough surfaces of the functionalized VGCNF are clearly indicative of modification with organic moieties (Figure 2). However, the average diameters of the functionalized VGCNF remained more or less unchanged (see Figure SS-1, Supporting Information). This is not unexpected since the average diameters of VGCNF (90−100 nm) is much larger than the molecular length of the pendant (ca. 1 nm from an AM1 modeling), and the increase would be too small to be observed by SEM.

The pristine VGCNF shows excellent thermal stability in both air and helium (Figure 3): in air, the unmodified VGCNF underwent a catastrophic weight loss at temperatures >700 °C, and was fairly stable up to 900 °C in helium. In the case of **6**, we expected that the onset of weight loss under either air or helium atmosphere should commence at much lower temperatures because of the organic pendants. Indeed, H_2N-VGCNF started to lose weight at 247 °C in air and 243 °C in helium, respectively, due to the decomposition of organic amine groups. The TGA curve taken in air showed a two-stage degradation process. H_2N-VGCNF lost 45.6% of weight between 250 and 700 °C, attributable to the loss of arylcarbonyl substituents, with 55.4% of residue at 700 °C due to VGCNF. It is important to point out that the subsequent degradation pattern of **6** is practically congruent with that of the unmodified VGCNF in the 700−900 °C region. On the basis of TGA and element analysis results (Table 1 and Figure 3), we tentatively concluded that there were approximately five arylcarbonyl groups[22] covalently attached to the nanofiber framework for every 100 carbon sites.

PPA-Treated VGCNF. For the purpose of probing the effect of PPA/P_2O_5 on VGCNF, a control experiment was run where VGCNF without TMPBA was heated in PPA/P_2O_5 at 130 °C for 3 days to afford a PPA-treated VGCNF (designated as PT-VGCNF, **7**) in 94% recovery yield. The workup was the same as that for H_2N-VGCNF. The IR spectrum of PT-VGCNF is essentially the same as that of the pristine VGCNF (see Figure

Scheme 1. Functionalization of VGCNF with 3-Aminophenoxy-4-benzoic Acid[a]

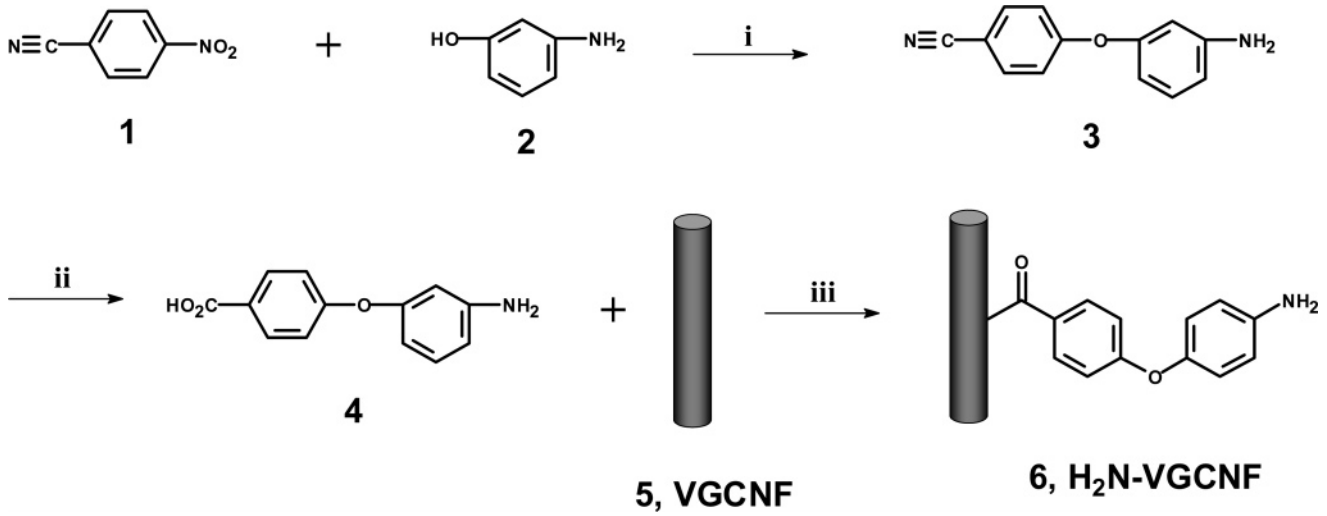

[a] Key: (i) NMP, K_2CO_3, 160 °C, 6 h. (ii) PPA, H_2O, 120 °C, 8 h. (iii) P_2O_5/PPA, 130 °C, 3 d.

Scheme 2. Synthesis of CP2-*g*-VGCNF Nanocomposites via in Situ Polymerization of 6FDA (8), APB (9) and H_2N-*g*-VGCNF (6)[a]

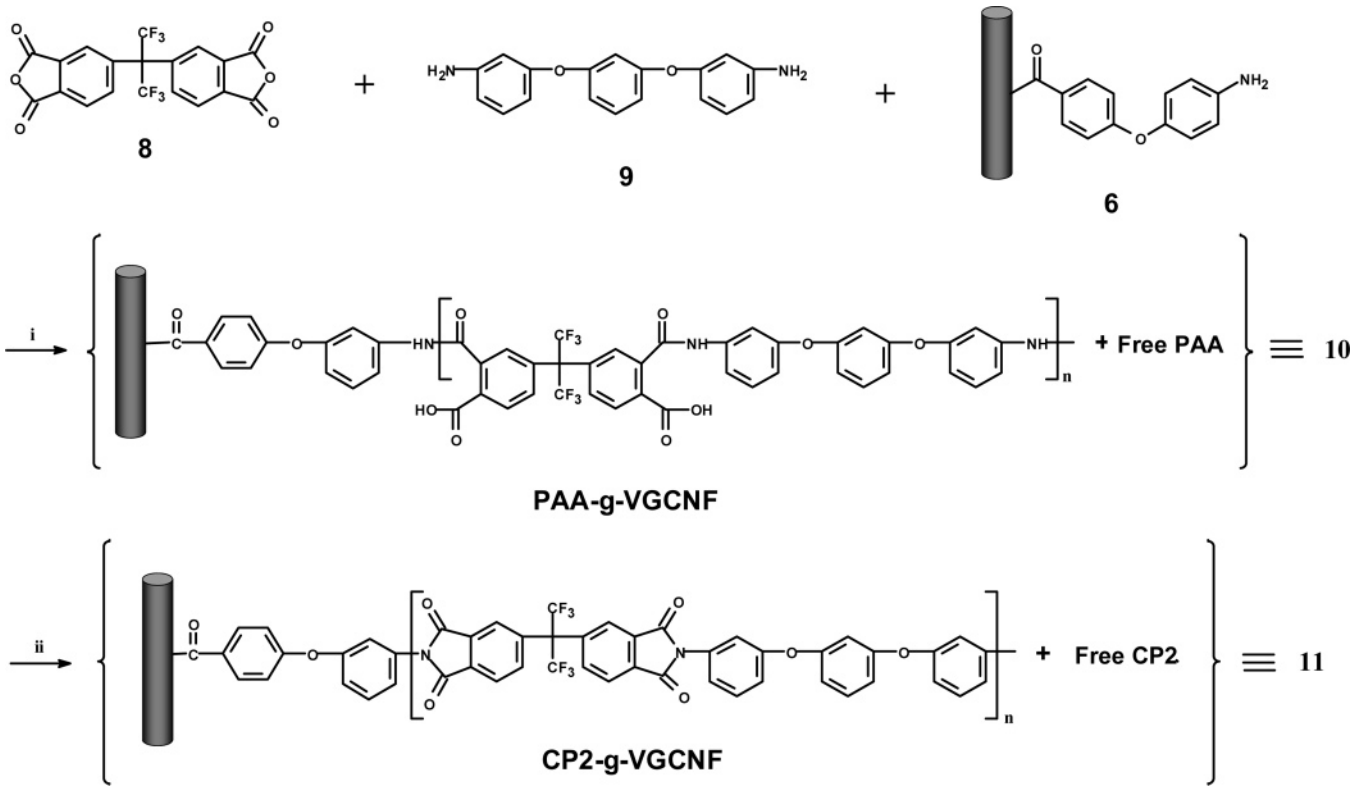

[a] Key: (i) DMAc, room temperature. (ii) 100 °C, 24 h; 150 °C, 4 h; 200 °C, 2 h; 250 °C, 1 h.

1). PT-VGCNF has slightly lower carbon and hydrogen contents than those of the pristine VGCNF (Table 1). In addition, both the pristine and PT-VGCNF share the same morphologies, including the surface texture, diameter and length (Figure 4). All these results reaffirm that PPA is indeed a mild, nondestructive medium for F−C reactions on carbon nanosurfaces.

Preparation and Characterization of CP2-*g*-VGCNF Nanocomposites and CP2/VGCNF Blends. The polymerization of the dianhydride 6FDA (**8**) and the diamine APB (**9**) was conducted in the presence of well-dispersed H_2N−VGCNF (**6**) in DMAc at room temperature for 24 h to afford poly(amic acid)-graft-nanofibers (PAA-*g*-VGCNF) that remained soluble in DMAc together with the free **PAA** (blends generically designated as **10** in Scheme 2). The resulting viscous and yellow solutions were diluted with DMAc, and then poured into a glass dish, followed by curing (imidization) at an elevated temperature to afford a series of CP2-*g*-VGCNF nanocomposite films (designated as **11** in Scheme 2). The VGCNF content (i.e, with respect to the weight of "formally unfunctionalized VGCNF" in the samples for valid property comparison with VGCNF/CP2 blends) in these CP2-*g*-VGCNF nanocomposite films was set at 0, 0.1, 0.3, 1.0, 2.0, and 5.0 wt %, corresponding to 0, 0.18, 0.55, 1.83, 3.68, and 9.19 wt % H_2N−VGCNF. In another set of another experiments, the as-received VGCNF was in attendance during the similarly conducted in situ polymerization of 6FDA (**8**) and APB (**9**) to afford the unattached PAA/VGCNF

Scheme 3. Preparation of VGCNF/CP2 Blends via in Situ Polymerization of 6FDA (8), APB (9) and Pristine VGCNF (5)[a]

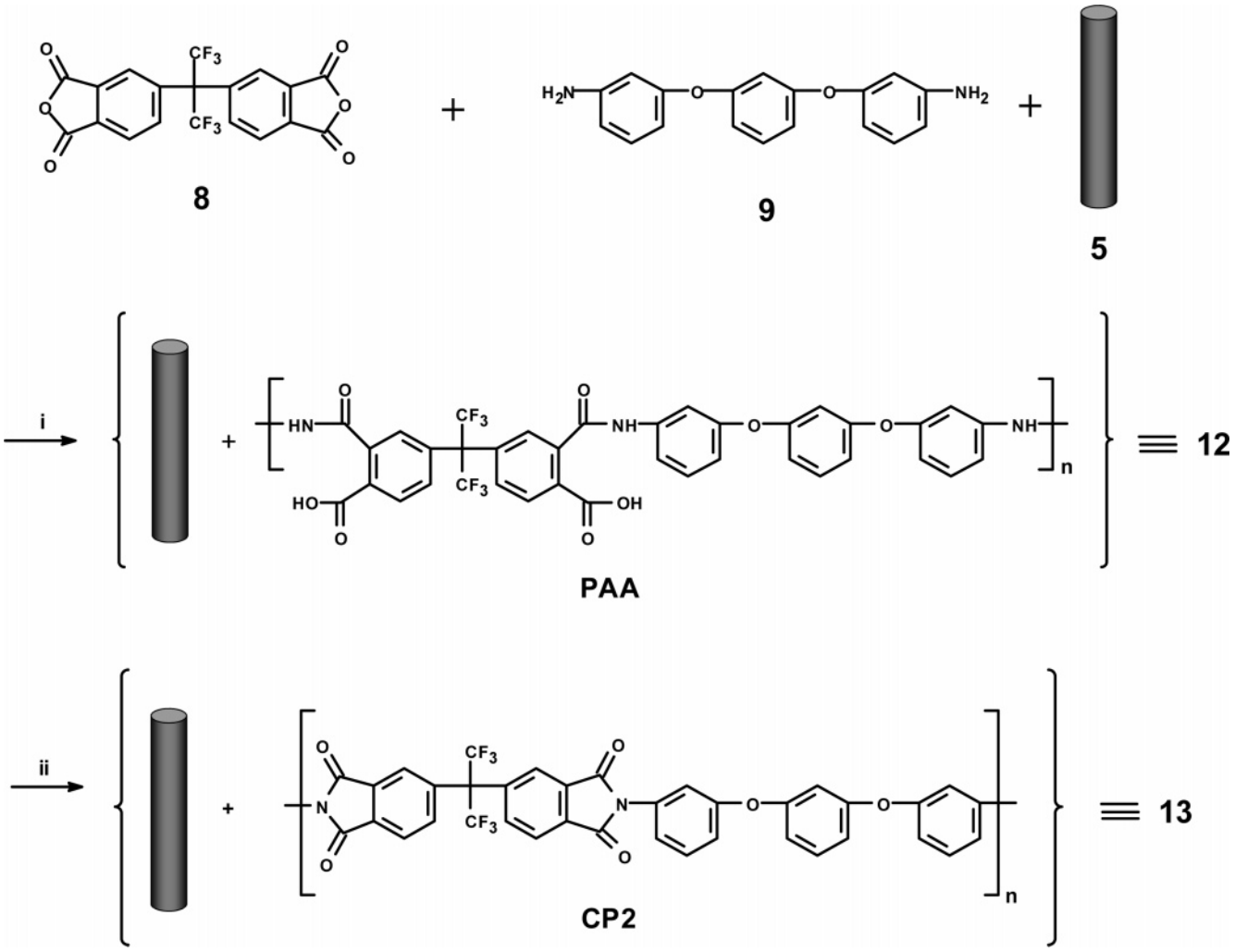

[a] Key: (i) DMAc, room temperature, 24 h. (ii) 100 °C, 24 h; 150 °C, 4 h; 200 °C, 2 h; 250 °C, 1 h.

solution (designated as **12** in Scheme 3), followed by the same curing (imidization) protocol as that previously used for CP2-*g*-VGCNF series to afford another series of CP2/VGCNFblend films (nanocomposites generically designated as **13** in Scheme 3) with the same VGCNF contents.

The similarly prepared, unfilled CP2 film is slightly yellow but optically transparent (Figure 5). The dispersion of 0.18 wt % H_2N-VGCNF (corresponding to 0.1 wt % VGCNF) in the CP2-*g*-VGCNF film is more uniform than the corresponding 0.1 wt % VGCNF in the CP2/VGCNF film, which contains visually large aggregates of VGCNF. The polymer film containing 0.55 wt % H_2N-VGCNF is still translucent while the films containing more than ca. 2 wt % H_2N-VGCNF have become opaque.

Solution Properties. In order to investigate the effect of VGCNF on the molecular weight (MW) of CP2, both CP2-*g*-VGCNF and CP2/VGCNF films were weighed and then immersed in THF for 2 days. Then, the mixtures were filtered through a 0.8 μm PTFE membrane and washed with large amount of THF. The filtrates containing extracted polyimide (i.e., THF-soluble CP2) were concentrated and the MWs were determined by gel-permeation chromatography (GPC) using polystyrene standards. The residual black solids or films were collected, dried and weighed to determine the "insoluble content in THF" values for Tables 2 and 3. It is reasonable to assume that the THF-insoluble fractions comprise the polymer-grafted VGCNF because the amounts are much larger than the respective VGCNF feed amounts and they were soluble in amide solvents and methanesulfonic acid (infra vida). The molecular weights of the polyimide grafts on VGCNF were calculated based on the assumption that there were five arylcarbonylation sites for every 100 carbons of the VGCNF (Table 1). The number-average (M_n) and weight-average (M_w) MWs of the neat CP2 are 84 200 and 238 400 Da, respectively. For CP2-*g*-VGCNF, the M_ns of THF-soluble CP2 increase to 126,300 Da with 0.1 wt % of VGCNF and then decrease gradually to 41,900 Da as VGCNF contents increase to 5.0 wt %. The MW of grafted CP2 is 5280 Da for 0.18 wt % CP2-*g*-VGCNF film and decrease to 2280 Da for 9.19 wt % film according to the calculation explained in Table 2. The decrease of molecular weights is due to the increase of amine-group numbers as the H_2N-VGCNF contents increase.

For CP2/VGCNF (blend) films, although the M_n of THF-soluble CP2 increase to 126,200 Da with 0.1 wt % of VGCNF, the M_n values decrease gradually to 57 090 Da as VGCNF contents increase to 5.0 wt %. The insoluble contents in THF for CP2/VGCNF are similar to the VGCNF contents, providing the evidence that there are practically no physically adsorbed CP2 in these blends (Table 3).

It seems that at the low concentration (0.1 wt % VGCNF), both pristine and functionalized VGCNFs increase the molecular weights of CP2. The viscosities of various poly(amic acids) have

Table 2. Molecular Weights and Molecular Distributions of CP2-*g*-VGCNF Nanocomposites

VGCNF content (wt %)	M_n[a]	M_w[a]	PDI[a]	insoluble content in THF (wt %)	content of CP2 grafted onto VGCNF (wt %)[b]	MW/chain[c]	DP/chain[d]
0 (0)[e]	84 200	238 400	2.83	0	0		
0.1 (0.18)[e]	126 200	371 300	2.94	2.3	2.2	5280	15.1
0.3 (0.55)[e]	91 400	238 600	2.61	6.1	5.8	4640	13.2
1.0 (1.83)[e]	55 600	146 200	2.63	15.4	14.4	3460	9.88
2.0 (3.68)[e]	56 780	135 700	2.39	30.9	28.9	3470	9.91
5.0 (9.19)[e]	41 900	94 300	2.25	52.5	47.5	2280	6.51

[a] Molecular weights and MW distributions of CP2 soluble in THF determined by size-exclusion liquid chromatography in THF. [b] Weight percentage of CP2 grafted onto VGCNF. It is equal to insoluble content in THF minus VGCNF content. [c] Molecular weights of CP2 insoluble in THF calculated by the following equation: MW/chain = (Content of CP2 grafted onto VGCNF)/((VGCNF content/12) × 0.05) where 0.05 is reactive-site fraction on H_2N-*g*-VGCNF (5 atom %). 12 is the carbon formula weight. [d] Degree of polymerization (DP)/chain = (MW/chain)/350.3 (fw of repeat unit: $C_{19.5}H_4F_3NO_3$). [e] The values for the wt % based on H_2N−VGCNF are in parentheses.

Table 3. Molecular Weights and Molecular Distributions of CP2/VGCNF Blends

VGCNF (wt %)	M_n[a]	M_w[a]	PDI[a]	insoluble content in THF (wt %)
0	84 200	238 400	2.83	0
0.1	126 200	415 600	3.29	0.10
0.3	85 200	198 000	2.33	0.33
1.0	62 060	154 100	2.63	1.06
2.0	70 530	153 700	2.18	1.88
5.0	57 090	128 460	2.25	5.32

[a] Molecular weights and molecular distributions (PDI) of CP2 soluble in THF measured by size-exclusion liquid chromatography in THF.

Table 4. Viscosity and Thermal Properties of CP2-*g*-VGCNF Nanocomposite Films

			TGA			
			in helium		in air	
VGCNF (wt %)	$[\eta]$[a] (dL/g)	DSC T_g[b] (°C)	$T_{d5\%}$[c] (°C)	char[d] (%)	$T_{d5\%}$[c] (°C)	char[d] (%)
0 (0)	0.42	199	530	56.5	526	1.14
0.1 (0.18)[e]	0.65	201	528	52.9	526	0.33
0.3 (0.55)[e]	0.94	202	531	55.7	520	0.38
1.0 (1,83)[e]	1.12	199	529	56.4	525	0.55
2.0 (3.68)[e]	1.37	197	525	56.5	520	0.51
5.0 (9.19)[e]	1.43	196	526	53.6	520	1.26

[a] Intrinsic viscosity measured in NMP at 30.0 ± 0.1 °C. [b] Inflection in baseline on DSC thermogram obtained in N_2 with a heating rate of 10 °C/min. [c] Temperature at which 5% weight loss recorded on TGA thermogram obtained with a heating rate of 10 °C/min. [d] Char yield at 850 °C. [e] The values for the wt% based on H_2N−VGCNF are in the parenthesis.

been reported to decrease over days after preparation. The initial high molecular weight could be resulted from the interfacial polymerization between the diamine and dianhydride monomers to form the poly(amic acid), which reequilibrated to lower molecular weights over a period of time.[23] It is possible that VGCNF promotes the interfacial polymerization at lower concentration during the preparation of poly(amic acid) or slows down the reequilibration, resulting in higher CP2 molecular weights. On the other hand, the decrease of molecular weight at higher VGCNF concentrations could be attributed to decreased mobility of the aromatic diamine, resulting from $\pi-\pi$ overlap interactions with VGCNF surface.[24] In the case of CP2-*g*-VGCNF, H_2N−VGCNF could have served as an end-capping agent during the in situ polymerization, and cause the stoichiometric imbalance between the diamine and dianhydride monomers, leading to lower MWs. Nevertheless, the molecular weights of all the CP2 extracts are higher than 40 000 Da, which are assumed to be high enough for the overall properties of CP2 to be unaffected.

Interestingly, the 5 wt % CP2-*g*-VGCNF nanocomposite film was swollen with little loss in its structural integrity after a 2-day of immersion in THF, whereas the similar CP2/VGCNF blend film disintegrated into powders due to the dissolution of CP2-polyimide in THF (Figure 6 and Figure SS-2). At first we suspected that CP2 formed cross-linked networks with H_2N−VGCNF and became solvent-resistant. However, we found that these nanocomposite films were soluble in stronger solvents such as DMAc, NMP, and methanesulfonic acid. In fact, the intrinsic viscosities of CP2-*g*-VGCNF nanocomposites were measured in NMP (Table 4). The viscosity of pristine CP2 is 0.42 dL/g while the viscosities of the nanocomposites increase from 0.65 to1.43 dL/g as the VGCNF contents increase from 0.1 to 5 wt %. Although the molecular weights of CP2-*g*-VGCNF decrease with the VGCNF contents, their viscosities increase due to the large aspect ratios of VGCNF.

Thermal Properties. The glass-transition (T_g) temperatures of CP2-*g*-VGCNF and CP2/VGCNF samples were determined by DSC. The film samples were heated to 300 °C in the DSC chamber in the first run and cooled to ambient temperature at 10 °C/min under nitrogen purge. Then the samples were heated to 300 °C at 10 °C/min in the second run. The T_g's were calculated based on midpoint of change in slope on the second heating run. In a previous work, we observed the T_g's of *m*-polyetherketone (*m*PEK) increased gradually with VGCNF contents after *m*PEK was grafted onto VGCNF.[10b] This is consistent with the rationale that the attachment of flexible *m*PEK chains to the rigid VGCNF surface imposes constraints over their mobility, resulting in increase in the glass-transition temperature. However, we observed some unusual thermal behaviors for both CP2-*g*-VGCNF and CP2/VGCNF films. The glass transition temperature of CP2-polyimide is 199 °C. The T_g values of 0.1 and 0.3 wt % CP2-*g*-VGCNF films increase to 201 and 202 °C, respectively. As the VGCNF contents were incrementally increased from 0.3 to 5 wt %, the T_g's of CP2-*g*-VGCNF films decrease from 201 to 196 °C (Table 4 and Figure 6a). The T_g's of CP2/VGCNF films change similarly to those of CP2-*g*-VGCNF films. The T_g of 0.1 wt % CP2/VGCNF film increased from 199 °C (CP2) to 203 °C. Then the T_g's decreased to 202 °C for 0.3 wt % CP2/VGCNF film, and further decreased to 194 °C as VGCNF contents increase to 5 wt % (Table 3 and Figure 6b). Since the M_n values of CP-*g*-VGCNF and CP2/VGCNF films are relatively high (>40 000 Da), it was unexpected that the T_g's decreased with VGCNF contents, too. A possible explanation invokes the presence of the microvoids formed between CP2 and VGCNF due to CP2 shrinkage during the thermal imidization process. The microvoids act collectively as free volume in the polymer matrix. As the free volume of a polymer increases, its T_g decreases.[25] Thus, as the number of microvoids (the overall size of free volume) increased with VGCNF contents, the glass transition of the CP2 polymer in the nanocomposites and physical blends was depressed accord

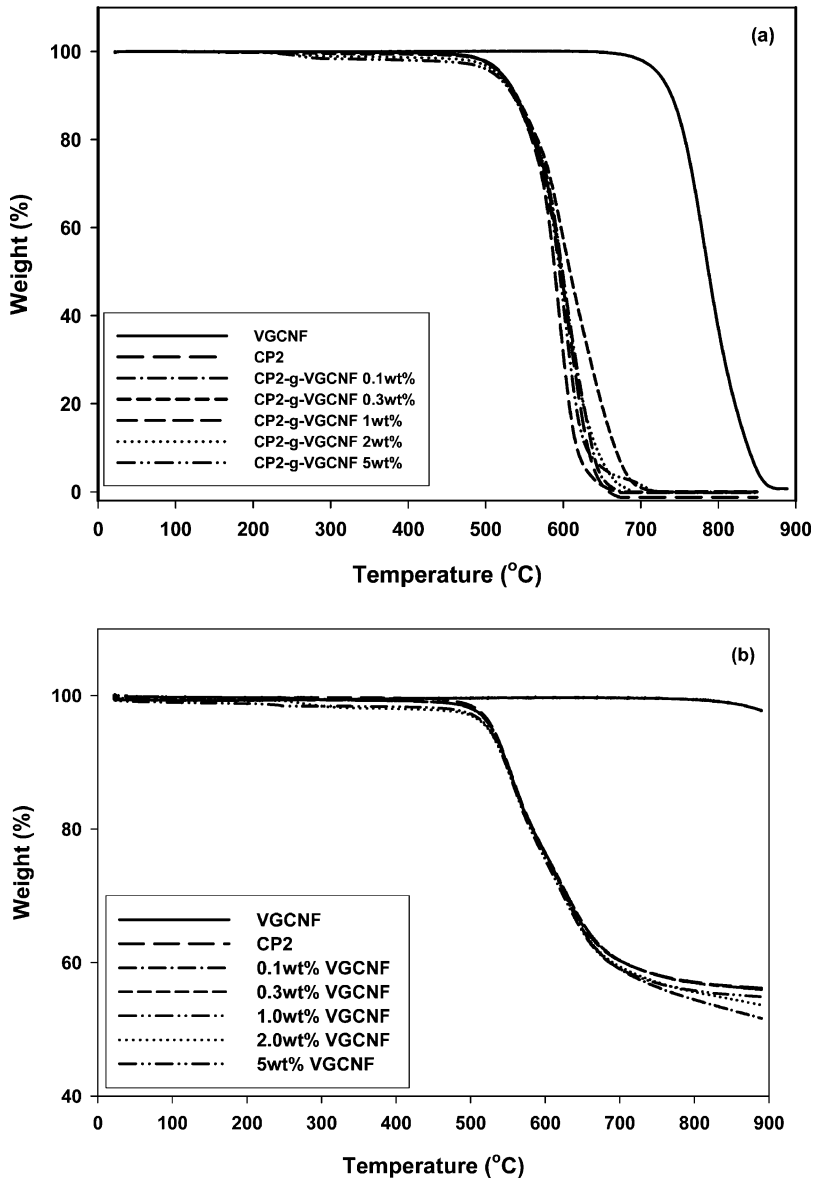

Figure 7. TGA thermograms of CP2-*g*-VGCNF with heating rate of 10 °C/min (a) in air and (b) in helium.

ingly. Watson et al. also observed T_g decreases with addition of CNTs and VGCNF into polyimides.[26] Similar results have been observed when nanoclay and bentonite were blended with epoxies and cyanate ester, respectively,[27] where the free volume fractions increased with the contents of nanoclay and bentonite. The T_g's of the resulting nanocomposites decreased accordingly in most occasions.

Thermogravimetry analysis (TGA) results showed that all the film samples exhibited excellent thermal and thermooxidative stabilities, with 5% weight loss temperature ranging from 524 to 531 °C in helium and 518−526 °C in air, respectively (Figure 7 and Tables 4 and 5).

Infrared Spectra. The films of CP2-polyimide, 5 wt % CP2-*g*-VGCNF nanocomposite, and 5 wt % CP2/VGCNF blend were subjected to attenuated total reflectance Fourier-transform infrared (ATR−FTIR) measurements. CP2 shows a strong absorption band at 1718 cm^{-1} and weak one at 1778 cm^{-1} attributable to the symmetric and asymmetric stretches of carbonyl groups in an imide ring. The peaks at 1587 and 1187 cm^{-1} are assigned to the stretches of carbon−carbon double bond in benzene rings and ether linkages of APB, respectively (see Figure SS-3 for the FT-IR spectra). In the CP2-*g*-VGCNF sample, the absorption bands in their IR spectrum generally became broader than those of the free CP2-polyimide. However, most major peaks of CP2 are still identifiable in the region of 1000−2000 cm^{-1}, but there is practically no absorption detectable below 1000 cm^{-1} region. After free CP2 has been removed by THF washing, the resulting IR peaks become broader and the absorption intensity is generally lower than before.

Table 5. Thermal Properties of CP2/VGCNF Blend Films

		TGA			
		in helium		in air	
VGCNF (wt %)	DSC T_g[a] (°C)	$T_{5\%}$[b] (°C)	char[c] (%)	$T_{5\%}$ (°C)	char (%)[c]
0	199	524	53.5	521	0.15
0.1	203	531	54.6	522	0.00
0.3	202	530	56.1	520	0.22
1.0	200	532	55.3	518	0.11
2.0	195	527	57.2	521	0.23
5.0	194	528	56.4	521	0.11

[a] Inflection in baseline on DSC thermogram obtained in N_2 with a heating rate of 10 °C/min. [b] Temperature at which 5% weight loss occurred on TGA thermogram obtained with a heating rate of 10 °C/min. [c] Char yield at 850 °C.

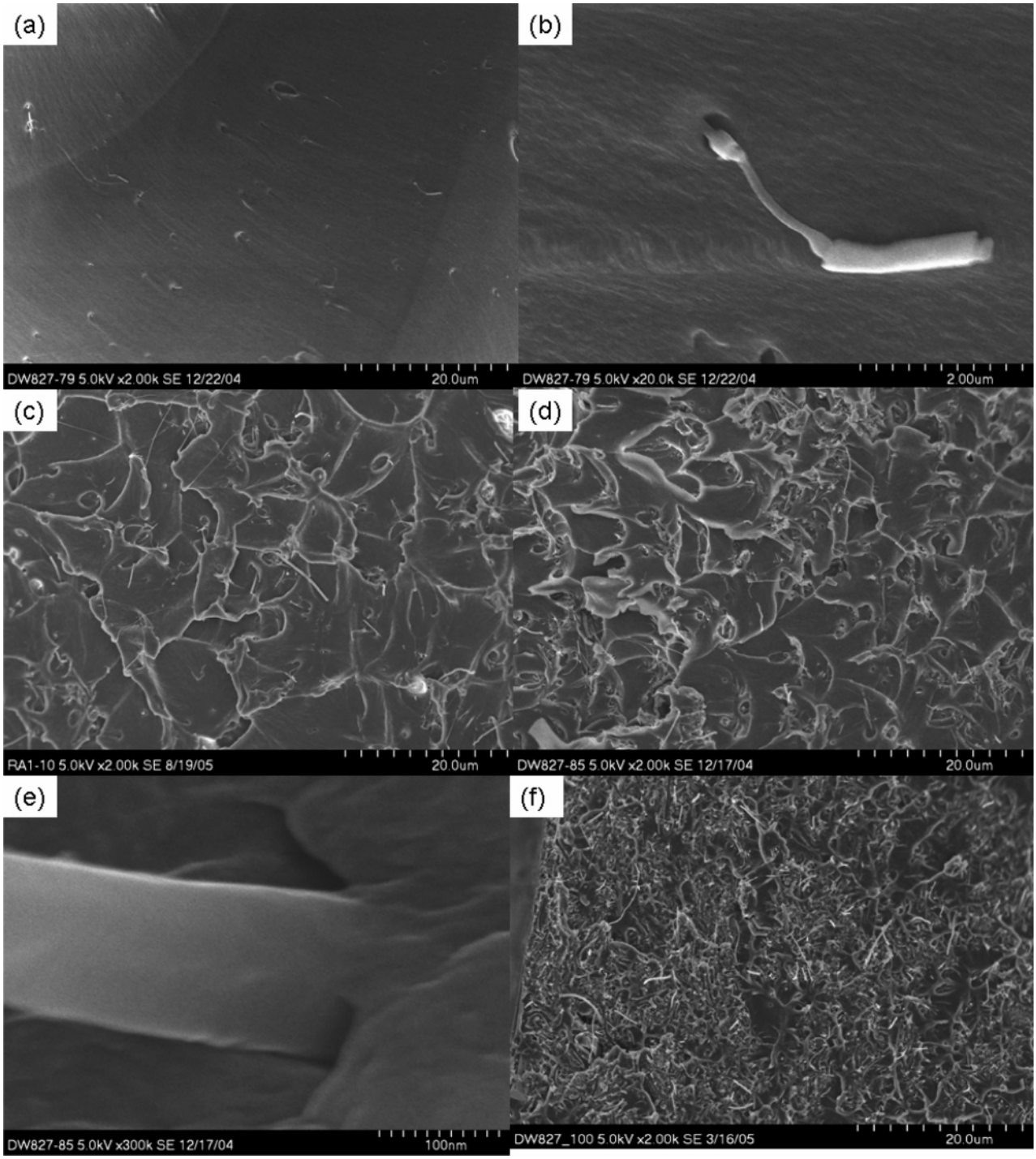

Figure 8. SEM images of CP2-*g*-VGCNF (a) 0.1 wt % VGCNF (×2k), (b) 0.1 wt % VGCNF (×20K), (c) 1.0 wt % VGCNF (×2k), (d) 2.0 wt % VGCNF (×2k), (e) 2.0 wt % VGCNF (×300K) and 5.0 wt % VGCNF (×2k).

On the other hand, the film of 5 wt % CP2/VGCNF blend exhibits essentially the same vibrational pattern as that of CP2 homopolymer. However, after the CP2/VGCNF film has been immersed in THF for 2 days, the near-quantitative removal (extraction) of CP2 from the sample is confirmed by the spectrum of the black residue, which shows that the vibrational bands characteristic of CP2 in 750−2000 cm^{-1} region have practically vanished. (see Figure SS-4 for the FT-IR spectrum).

Scanning Electron Microscope (SEM). High-resolution SEM was used to evaluate the dispersion of the carbon nanofibers in CP2-polyimide matrix. The nanofibers of 0.1 wt % CP2-*g*-VGCNF are dispersed well in the polyimide matrix as shown in Figure 8a. Higher resolution SEM images revealed that the nanofibers were coated with the polymers and their diameters had increased roughly by 100−300 nm (Figure 8b). The 1, 2, and 5 wt % CP2-*g*-VGCNF films also display relatively uniform dispersion (Figure 8, parts c, d, and f). The good interfacial adhesion as manifested by continuity between CP2 and VGCNF is also observed (Figure 8e). However, the dispersion of the pristine VGCNF in CP2 is not as good as the functionalized VGCNF. The 2 wt % CP2/VGCNF film shows uniform dispersion in one area (Figure 9a) and large aggregates in other area (Figure 9b).

Mechanical Properties. The nanocomposite films were cut into 50 × 5 mm slices and a Tinius Olsen tensometer was used to measure their tensile properties with a crosshead separation

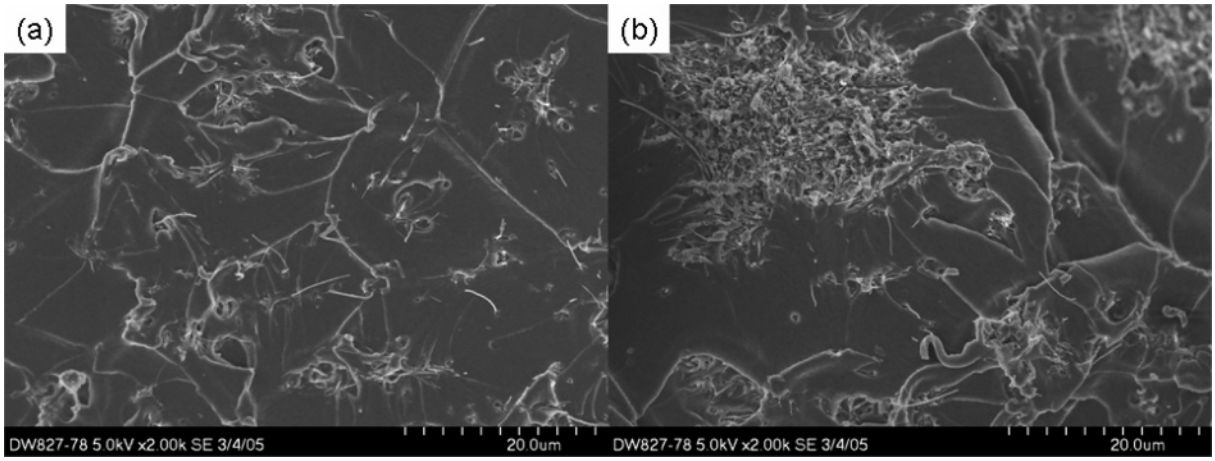

Figure 9. SEM images of CP2/VGCNF (a) 2.0 wt % VGCNF (×2k) and (b) 2.0 wt % VGCNF (×2k).

Table 6. Thin Film Tensile Properties of CP2-*g*-VGCNF Nanocomposites

VGCNF (wt %)	tensile strength (MPa)	tensile modulus (GPa)	tensile strain (%)
0	116 ± 5	3.3 ± 0.2	6.3 ± 1.1
0.1	120 ± 11	3.5 ± 0.1	6.2 ± 0.5
0.3	126 ± 11	3.6 ± 0.2	6.4 ± 0.7
1.0	131 ± 7	3.5 ± 0.2	6.2 ± 1.2
2.0	122 ± 5	3.7 ± 0.2	4.7 ± 0.6
5.0	124 ± 5	4.8 ± 0.4	5.9 ± 0.8

Table 7. Thin Film Tensile Properties of CP2/VGCNF Blends

VGCNF (wt %)	tensile strength (MPa)	tensile modulus (GPa)	tensile strain (%)
0	116 ± 5	3.3 ± 0.2	6.3 ± 1.1
0.1	84.4 ± 10.8	2.9 ± 0.2	5.1 ± 0.3
0.3	102 ± 13	3.1 ± 0.4	4.6 ± 0.3
1.0	96.5 ± 13.1	3.2 ± 0.3	5.0 ± 0.5
2.0	87.5 ± 11.4	3.0 ± 0.2	4.2 ± 0.6
5.0	52.1 ± 6.4	2.6 ± 0.3	2.3 ± 0.2

speed of 1 mm/min. As shown in Table 6, both the tensile strength and strain of CP2-*g*-VGCNF films increase as VGCNF content is increased from 0 to 5 wt %, indicating that the stiffness of nanocomposite films is directly increased with VGCNF content. The modulus increases from 3.3 to 4.8 GPa (a 45% increase) as the VGCNF contents increased from 0 to 5 wt % while the tensile strengths increase moderately. The cross sections of the thin films were examined with high-resolution SEM (see Figure SS-5 for HR−SEM image). Some nanofibers are broken under the stress, which indicates the good adhesion with the polymer matrix. Some simply are pulled out, leaving holes in the CP2 matrix, indicative of poor adhesion between the fibers and polymer matrix. On the other hand, the tensile strength, strain, and modulus of CP2/VGCNF films are lower than those of the pristine CP2 film (Table 7). The poor dispersion of the pristine VGCNF in CP2 together with the poor adhesion between them could contribute to the resulting lower mechanical properties of CP2/VGCNF films. The VGCNF aggregate appearing in Figure 10b can act as a defect instead of as a reinforcement. It is worth noting that the several reported in situ syntheses of MWNT−polyimide nanocomposites had led to improvement in mechanical properties in various degrees. For example, Jiang et al. reported that the mechanical properties of the polyimide- (Kapton-) based in situ nanocomposites were not improved significantly by the addition of pristine MWNTs. Young's modulus had increased only 6% with 1.89 vol % of MWNT, but decreased when the MWNT content was further increased,[28] whereas Ge et al. claimed significant improvement

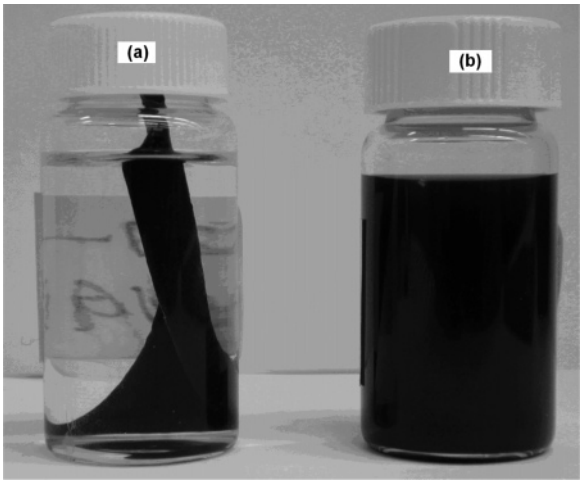

Figure 10. VGCNF-containing CP2 films during 2-day immersion in THF: (a) 5 wt % CP2-*g*-VGCNF nanocomposite; (b) 5 wt % CP2/VGCNF blend.

for their MWNT−poly(ether imide) nanocomposites: 8−60% increase in tensile strength and 28−25% in modulus for a MWNT content of 0.14−0.38 wt %.[29]

Conclusion

In this work, we have shown that an amine-containing benzoic acid could be used to arylcarbonylate vapor grown carbon nanofibers and multiwalled carbon nanotubes via a Friedal-Crafts acylation reaction in an optimized PPA/P_2O_5 medium.[30] We believe this is the first example of carbon nanofibers that contain aromatic amines capable of further reactions under appropriate conditions. The resulting H_2N−VGCNF with relatively high degree of functionalization was able to participate in the in situ polymerization of a dianhydride (6FDA) and a diamine (APB) to afford, after typical thermal curing, a series of polyimide-based nanocomposite (CP2-*g*-VGCNF) films, which contained 0.1 to 5 wt % of the functionalized VGCNF. Therefore, while our previous work has shown the feasibility of directly grafting the defect sites on either VGCNF or MWNT via a Friedel−Crafts acylation reaction in poly(phosphoric acid) with a suitable, arylether−benzoic acid type AB or AB_2 monomer in a one-pot fashion, this work further demonstrates the feasibility of in situ grafting of prefunctionalized VGCNF (most likely MWNT as well) with a well-studied aromatic polyimide (CP2) under the conventional AA + BB polymerization and thermal (solid-state) imidization conditions. In this two-stage preparation of in situ nanocomposites, the presence

of prefunctionalized VGCNF has little or no adverse effect on the molecular weight of the resulting polyimide. However, based on the comparative results from solvent extraction experiments, there was more free polyimide present in nanocomposites described here than there were free poly(ether ketone)s in the previous cases.[10b,e,f] This may be arisen from the kinetics of polymerization. Last but not least, we confirm that the functionalized VGCNF has a better dispersion in and a stronger bonding with the matrix polymer in the CP2 films than the unfunctionalized counterpart, as evidenced by the better mechanical properties, THF-extraction results, and the comparison of SEM data. The electrical response of these nanocomposite films has also been investigated for use as high-temperature electrostatic dissipation (ESD) and electromagnetic interference (EMI) shielding films and as thermal electric switches. The details of the results and discussion will be presented elsewhere.[31]

Acknowledgment. We thank Gary Price and Marlene Houtz (University of Dayton Research Institute) for SEM images and TGA data, respectively. This project was supported by funding from Wright Brother Institute (Dayton), Office of Scientific Research (AFOSR) and Materials & Manufacturing Directorate, US Air Force Research Laboratory. We thank the reviewers for helpful comments.

Supporting Information Available: (i) Figure SS-1, SEM images of (a) as-received VGCNF (×25K) and (b) H_2N−VGCNF (×250K), indicating that the CNF diameters remained more or less the same; (ii) Figure SS-2, VGCNF-containing CP2 films recovered after extended immersion in THF, (a) 5 wt % CP2-*g*-VGCNF and (b) 5 wt % CP2/VGCNF blend; (iii) Figure SS-3, IR spectra of (a) CP2 film, (b) 5 wt % CP2-*g*-VGCNF nanocomposite film before THF extraction, and (c) 5 wt % CP2-*g*-VGCNF nanocomposite film after THF extraction; Figure SS-4; IR spectra of (a) CP2 film, (b) 5 wt % CP2/VGCNF blend film before THF extraction, and (c) 5 wt % CP2/VGCNF powder after THF extraction.; (iv) Figure SS-5, SEM image of 0.1 wt % CP2-*g*-VGCNF after Instron testing (×50K). This material is available free of charge via the Internet at http://pubs.acs.org.

References and Notes

(1) Maruyama, B.; Alam, K. *SAMPE J.* **2002**, *38* (3), 59−70.
(2) Koerner, H.; Liu, W.; Alexander, M.; Mirau, P.; Dowty, H.; Vaia, R. A. *Polymer* **2005**, *46*, 4405−4420.
(3) Tasis, D.; Tagmatarchis, N.; Bianco, A.; Prato, M. Chemistry of Carbon Nanotubes. *Chem. Rev.* **2006**, *106*, 1105−1136.
(4) Chen, J.; Hamon, M. A.; Hu, H.; Chen, Y.; Rao, A. M.; Eklund, P. C.; Haddon, R. C. *Science* **1998**, *282*, 95.
(5) Bahr, J. L.; Mickelson, E. T.; Bronikowski, M. J.; Smalley, R. E.; Tour, J. M. *Chem. Commun.* **2001**, *3*, 193.
(6) Dyke, C. A.; Tour, J. M. *J. Am. Chem. Soc.* **2003**, *125*, 1156.
(7) Khabashesku, V. N.; Billups, W. E.; Margrave, J. L. *Acc. Chem. Res.* **2002**, *35*, 1087.
(8) Peng, H.; Alemany, L. B.; Margrave, J. L.; Khabashesku, V. N *J. Am. Chem. Soc.* **2003**, *125*, 15174.
(9) (a) Winey, K. I.; Vaia, R. A. *MRS Bull.* **2007**, *32*, 314. (b) Moniruzzaman, M.; Winey, K. I. *Macromolecules* **2006**, *39*, 5194.
(10) (a) Baek, J.-B.; Lyons, C. B.; Tan, L.-S. *J. Mater. Chem.* **2004**, *14*, 2052. (b) Baek, J.-B.; Lyons, C. B.; Tan, L.-S. *Macromolecules* **2004**, *37*, 8278. (c) Baek, J.-B.; Park, S. Y.; Price, G. E.; Lyons, C. B.; Tan, L. S. *Polymer* **2004**, *46*, 1543. (d) Lee, H.-J.; Oh, S.-J.; Choi, J.-Y.; Kim, J. W.; Han, J.; Tan, L.-S.; Baek, J.-B. *Chem. Mater.* **2005**, *17*, 5057−5064. (e) Oh, S.-J.; Lee, H.-J.; Keum, D.-K.; Lee, S.-W.; Wang, D. H.; Park, S.-Y.; Tan, L.-S.; Baek, J.-B. *Polymer* **2006**, *47*, 1132−1140. (f) Wang, D. H.; Baek, J.-B.; Tan, L.-S. *Mater. Sci. Eng., B.* **2006**, *132*, 103.
(11) (a) Wei, G.; Fujiki, K.; Saitoh, H.; Shirai, K.; Tsubokawa, N. *Polym. J. (Tokyo)* **2004**, *36*, 316−322. (b) Wei, G.; Saitoh, S.; Saitoh, H.; Fujiki, K.; Yamauchi, T.; Tsubokawa, N. *Polymer* **2004**, *45*, 8723−8730. (c) Wei, G.; Shirai, K.; Fujiki, K.; Saitoh, H.; Yamauchi, T.; Tsubokawa, N. *Carbon* **2004**, *42*, 1923−1929.
(12) (a) Wilson, D.; Stenzenberger, H. D.; Hergenrother, P. M. *Polyimides*; Chapman and Hall: New York, 1990; pp 1−78. (b) Hergenrother, P. M. *Pays-Bas.* **1991**, *110*, 481. (c) Hergenrother, P. M. In *Polyimides and Other High-Temperature Polymers*; Abadie, M. J. M., Sillion, B., Ed.; Elsevier: New York, 1991; pp 1−18. (d) Critchley, J. P.; Knight, G. J.; Wright, W. W. *Heat Resistant Polymers*; Plenum Press: New York, 1983; pp 186−258. (e) Sroog, C. E. *J. Polym. Sci., Macromol. Rev.* **1976**, *11*, 161. (f) Cheng, S. Z. D.; Li, F.; Savitski, E. P.; Harris, F. W. *Trends Polym. Sci.* **1997**, *5*, 51.
(13) CP2 is shortened from the original acronym LARC-CP2, which originated from a NASA research program on colorless polymides (CP) for coating applications, where optical transparency was critical: (a) St. Clair, A. K.; St. Clair, T. L.; Shevket, K. I. *Polym. Mater. Sci. Eng.* **1984**, *51*, 62. (b) Miner, G. A.; Stoakley, D. M.; St. Clair, A. K.; Gierow, P. A.; Bates, K. *Polym. Mater. Sci. Eng.* **1997**, *76*, 381−382.
(14) (a) Yu, A.; Hu, H.; Bekyarova, E.; Itkis, M. E.; Gao, J.; Zhao, B.; Haddon, R. C. *Compos. Sci. Technol.* **2006**, *66*, 1190−1197. (b) Delozier, D. M.; Tigelaar, D. M.; Watson, K. A.; Smith, J. G.; Klein, D. J.; Lillehei, P. T.; Connell, J. W. *Polymer* **2005**, *46*, 2506−2521. (c) Delozier, D. M.; Watson, K. A.; Smith, J. G.; Connell, J. W. *Compos. Sci. Technol.* **2005**, *65*, 749−755. (d) Styers-Barnett, D. J.; Ellison, S. P.; Park, C.; Wise, K. E.; Papanikolas, J. M. *J. Phys. Chem. A* **2005**, *109*, 289−292. (e) Grujicic, M.; Cao, G.; Roy, W. N. *J. Mater. Sci.* **2004**, *39*, 4441−4449. (f) Delozier, D. M.; Tigelaar, D. M.; Watson, K. A.; Smith, J. G., Jr.; Lillehei, P. T.; Connell, J. W. *Int. SAMPE Symp. Exhib.* **2004**, *49* (SAMPE 2004), 2139−2151. (g) Qu, L.; Lin, Y.; Hill, D. E.; Zhou, B.; Wang, W.; Sun, X.; Kitaygorodskiy, A.; Suarez, M.; Connell, J. W.; Allard, L. F.; Sun, Y.-P. *Macromolecules* **2004**, *37*, 6055−6060. (h) Odegard, G. M.; Gates, T. S.; Wise, K. E.; Park, C.; Siochi, E. J. *Compos. Sci. Technol.* **2003**, *63*, 1671−1687. (i) Smith, J. G., Jr.; Watson, K. A.; Thompson, C. M.; Connell, J. W. *Int. SAMPE Tech. Conf.* **2002**, *34*, 365−376.
(15) Carneiro, O. S.; Covas, J. A.; Bernardo, C. A.; Caldeira, G.; Hattum, F. W. J. V.; Ting, J. M.; Alig, R. L.; Lake, M. L. *Compos. Sci. Technol.* **1998**, *58*, 401−407.
(16) Singh, C.; Quested, T.; Boothroyd, C. B.; Thomas, P.; Kinloch, I. A.; Abou-Kandil, A. I.; Windle, A. H. *J. Phys. Chem. B* **2002**, *106*, 10915−10922.
(17) CHRISKEV Company, Inc., 5109 W. 111th Terrace, Leawood, KS 66211−1742.
(18) (A) Schramm, J.; Radlmann, E.; Lohwasser, H.; N.ischk, G. *J. Liebigs Ann. Chem.* **1970**, *740*, 169. (b) Dann, O.; Fick, H.; Pietzner, B.; Walkenhorst, E.; Fernbach, R.; Zeh, D. *J. Liebigs Ann. Chem.* **1975**, *1*, 160. (c) Benson, D. A.; Karsch-Mizrachi, I.; Lipman, D. J.; Ostell, J.; Rapp, B. A.; Wheeler, D. L. *Genbank. Nucleic Acids Res.* **2000**, *28*, 15.
(19) Irwin, R. S. US Patent 5,395,917, 1995.
(20) Baek, J.-B.; Tan, L.-S. *Polymer* **2003**, *44*, 4135.
(21) (a) Li, J.; Vergne, M. J.; Mowles, E. D.; Zhong, W.-H.; Hercules, D. M.; Lukehart, C. M. *Carbon* **2005**, *43*, 2883. (b) Baker, S. E.; Tse, K.-Y.; Hindin, E.; Nichols, B. M.; Clare, T. L.; Hamers, Robert, J. *Chem. Mater.* **2005**, *17*, 4971. (c) Saeed, K.; Park, S.-Y.; Lee, H.-J.; Baek, J.-B.; Huh, W.-S. *Polymer* **2006**, *47*, 8019. (d) Wang, Y.; Iqbal, Z.; Malhotra, S. V. *Chem. Phys. Lett.* **2005**, *402*, 96.
(22) As pointed out by a reviewer, this value may be higher than the percentage of carbons on the outermost layer of a perfect MWNT. Since we had rigorously removed the residual, unreacted 3-aminophenoxy-4-benzoic acid **4** from the functionalized VGCNF product and our TGA experiment was reproducible, we could only speculate that the defects on the outermost layer of VGCNF might have allowed the access of the Friedel-Crafts reactant to the layer(s) underneath.
(23) (a) Volksen, W.; Cotts, P. M. In *Polyimides*; Mittal, K. L., Ed.; Plenum Press: New York, 1984; Vol 1, p 163. (b) Walker, C. C. *J. Polym. Sci., Part A: Polym. Chem.* **1985**, *30*, 3037.
(24) (a) Curran, S.; Ajayan, P. M.; Blau, W.; Carroll, D. L.; Coleman, J. N.; Dalton, A. B.; Davey, A. P.; Drury, A.; McCarthy, B.; Strevens, A. *Adv. Mater.* **1998**, *10*, 1091. (b) Chen, R. J.; Zhang, Y.; Wang, D.; Dai, H. *J. Am. Chem. Soc.* **2001**, *123*, 3838.
(25) (a) Ueberreiter, K.; Kanig, G. J. *Colloid Sci.* **1952**, *7*, 569. (b) Fox, T. G. *Bull. Am. Phys. Soc.* **1956**, *1*, 123. (c) Cohen, M. H.; Turnbull, D. *J. Chem. Phys.* **1959**, *31*, 1164.
(26) Watson, K. A.; Smith, J. G.; Connell, J. W. *Int. SAMPE Tech. Conf.* **2001**, *33*, 1551−1560.
(27) (a) Becker, O.; Cheng, Y.-B.; Valey, R. J.; Simon, G. P. *Macromolecules* **2003**, *36*, 1616; (b) Yu, D. H.; Wang, B.; Feng, Y.; Fang, Z. P. *J. Appl. Polym. Sci.* **2006**, *102*, 1509.
(28) Jiang, X.; Bin, Y.; Matsou, M. *Polymer* **2005**, *46*, 7418−7424.
(29) Ge, J. J.; Zhang, D.; Li, Q.; Hou, H.; Graham, M. J.; Dai, L.; Harris, F.; Cheng, S. Z. D. *J. Am. Chem. Soc.* **2005**, *127*, 9984−9985.
(30) We have confirmed that this method is also applicable to MWNT; results to be published.
(31) Arlen, M. J.; Wang, D. H.; Tan, L.-S.; Vaia, R. A. To be submitted for publication.

MA070157C